Extension of a Suspended Soap Film: A Homogeneous Dilatation Followed by New Film Extraction

Jacopo Seiwert, Martin Monloubou, Benjamin Dollet, and Isabelle Cantat

Institut de Physique de Rennes, UMR 6251 CNRS/Université de Rennes 1, 35042 Rennes Cedex, France
(Received 2 April 2013; published 26 August 2013)

Liquid foams are widely used in industry for their high effective viscosity, whose local origin is still unclear. This Letter presents new results on the extension of a suspended soap film, in a configuration mimicking the elementary deformation occurring during foam shearing. We evidence a surprising two-step evolution: the film first extends homogeneously, then its extension stops, and a new thicker film is extracted from the meniscus. The second step is independent of the nature of the surfactant solution, whereas the initial extension is only observed for surfactant solutions with negligible dilatational moduli. We predict this complex behavior using a model based on Frankel's theory and on interface rigidification induced by confinement.

Liquid foams are very dissipative materials, with an exceptionally high ratio between their effective viscosity and their density. For this reason, they are widely used for blast wave mitigation [1,2] or as drilling fluid in the oil industry [3], among other examples. However, the local processes leading to this high energy dissipation have not been entirely elucidated yet [4]. The dissipation rate is strongly enhanced by the confinement of the viscous liquid phase in thin films and menisci and it is extremely sensitive to the interfacial properties. Consequently, it depends on the local film thickness and on the interfacial stresses and velocities, acting as boundary conditions for the flows. These quantities are in practice impossible to measure *in situ* in a 3D sheared foam, making the prediction of the dissipation rate in such a system particularly challenging.

Local flow models at the bubble scale have been developed, leading to predictions at the foam scale which can be compared to experimental data [5–8]. However, direct measurements of the film thicknesses or deformations at the bubble scale are still sparse [9–15], although they are necessary to discriminate the very different assumptions made by the models on the local flow. Recent studies have established the relation between the interfacial rheology of foaming solutions and the bulk rheology of foams [16–18]. Interfacial rheology may be characterized by a dilatational modulus E_d, which relates relative interface area variations to interfacial stresses and which can span several orders of magnitude. Two limiting cases are traditionally considered: (i) "Rigid" surfactants feature large values of E_d (when compared to the surface tension) and exhibit incompressible interfaces [19], while (ii) "mobile" surfactants exhibit stress-free interfaces.

Physically, interfacial stresses mainly arise because stretching (or compressing) an interface leads to changes in the interfacial concentration of surfactants and hence to surface tension gradients. These gradients relax through the exchange of surfactants between the interface and the bulk, whose typical time scale depends on several processes: adsorption or desorption of surfactant molecules, diffusion, micelle dynamics, etc. E_d is thus not an intrinsic property of the solution but depends on the time and space scales of the method of measurement. From a practical standpoint, it is still unclear which of these two limiting models (incompressible and stress free), if any, will apply for a given experimental situation and a given surfactant solution because the relevant value of E_d is in general unknown.

Film area increase is one of the key processes occurring during foam shearing, along with film formation (after a bubble rearrangement), film shearing, and film area decrease. The linear response of a liquid film under oscillatory extensional strain has been precisely measured [11,20], but large extensional deformations involve entirely different, nonlinear processes which are the scope of this Letter. We show that the area increase of a preexisting thin film subjected to a large extension is mainly due to the extraction of a fresh film from the meniscus and not to an uniform extension of the preexisting film. The fresh film thickness quantitatively obeys Frankel's law, which quantifies the extraction of a soap film from a bath, assuming incompressible interfaces [21]. This behavior is observed for all tested surfactant solutions, independently of their dilatational moduli. However, the area of the preexisting film slightly increases during a first step, with a relative area variation that strongly depends on the nature and on the concentration of the surfactants. We argue that this initial extension modifies the surface tension in the film and thus produces the resistance required to pull the Frankel's film out of the meniscus. This two-step process evidences a transition between a compressible behavior of the interfaces at small strain and an incompressible behavior at
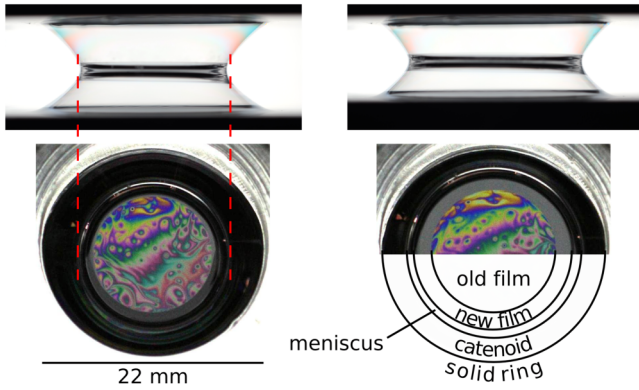
FIG. 1 (color online).   Top: side view of the experiment before (left) and during (right) stage motion. The darker band in the center of the image is the Plateau border. Bottom: corresponding top views, under white illumination (used for illustration: the thickness measurements are made with monochromatic light). It shows the old thin film with heterogeneous bright colors, surrounded by the thicker new film that appears uniformly gray.

larger strain for solutions usually leading to mobile interfaces without measurable resistance to compression or dilatation.

The experimental setup, shown in Fig. 1, features three axisymmetric soap films: a circular horizontal film which we study and two catenoids used to suspend it between two metallic circular rings (22 mm in diameter). The radius of the horizontal film increases when the distance between the rings decreases [11,22]. These three films meet at a meniscus (Plateau border), as within liquid foams.

A typical experiment proceeds as follows: the films are created, then let at rest. The Laplace pressure in the Plateau border is lower than in the flat thin films because the Plateau border is concave, inducing slow film drainage. The horizontal film thickness reaches a quasiuniform value h_0, in the range 0.5–1.5 μm, after typically 20–60 s. The horizontal film radius R is then increased from 7 to 10 mm by moving the lower ring at a constant velocity U_s in the range 0.05–50 mm/s. The lateral film profile is monitored by a first camera (see Fig. 1, top). The interference pattern produced in the horizontal film by a monochromatic lamp is recorded with a second camera (Fig. 1, bottom), giving a time-resolved map of the relative thickness of the film. A local absolute thickness reference is provided by a synchronized reflective interferometer. Additionally, the small thickness fluctuations act as passive tracers [23]

and provide qualitative information on the velocity field in the film.

The radius of curvature r_m of the Plateau border was varied between 0.2 and 2.0 mm by adding or withdrawing liquid with a syringe. We used three solutions ($T3$, $T13$, and $T25$; see Table I) with tetradecyltrimethylammonium bromide (TTAB) as a surfactant. TTAB is a soluble surfactant and has a typical adsorption time of 3 ms [12], which leads to mobile interfaces in most foam experiments. The fourth solution used a mixture of sodium lauryl-dioxyethylene sulfate (SLES), cocoamidopropyl betaine (CAPB), and myristic acid (MAc), specifically developed to produce rigid interfaces. Measures with the oscillating bubble method give $E_d < 1$ mN/m for (T) solutions and $E_d = 320$ at 0.2 Hz for (D) [12,19].

Upon retraction of the Plateau border, two successive regimes, schematized in Fig. 2, are observed when using the TTAB solutions. During the first step ($0 < t < t_e$), the film initially present (thereafter denoted "old film") undergoes a homogeneous extension, as attested by the motion of the thickness fluctuations. For $t > t_e$ (second step), the old film extension ceases and the subsequent increase in area is entirely compensated for by a thicker film extracted from the Plateau border, denoted "new film." This new film consists of a transition region of characteristic length l, followed by a region of length l_F and of approximately constant thickness, with a smooth maximum h^*. As observed in Fig. 1 (bottom right), these old and new films are well distinguishable during the entire experiment, and the film radius R can be decomposed unambiguously into three terms $R = r + l + l_F$, with r the old film radius. For the solution (D), only the second step has been observed.

Let us first focus on the new film. We measured h^* while varying systematically U_s and r_m for the different solutions. Figure 3 shows that it strictly obeys $h^* = h_F$, with $h_F = 2.68 r_m \text{Ca}^{2/3}$ the thickness predicted by Frankel [21]. Here, $\text{Ca} = \eta U/\gamma$ is the Capillary number and U the meniscus velocity. Although Frankel's law has been observed previously when a soap film is withdrawn from a liquid bath, our measurements are to our knowledge the first made in a configuration relevant to foams, with Plateau borders as liquid reservoir. In particular, the radius of the Plateau border r_m was varied over a decade.

The film of maximal thickness h^* is extracted from the Plateau border at time t^*. $\text{Ca}^* = \eta U(t^*)/\gamma$ is measured at

TABLE I.   Solutions properties. Glycerol (10 vol%) is added to every solution, leading to a viscosity $\eta = 1.4$ mPa s. The TTAB critical micelle concentration (c_{cmc}) is 3.8 mmol/L.

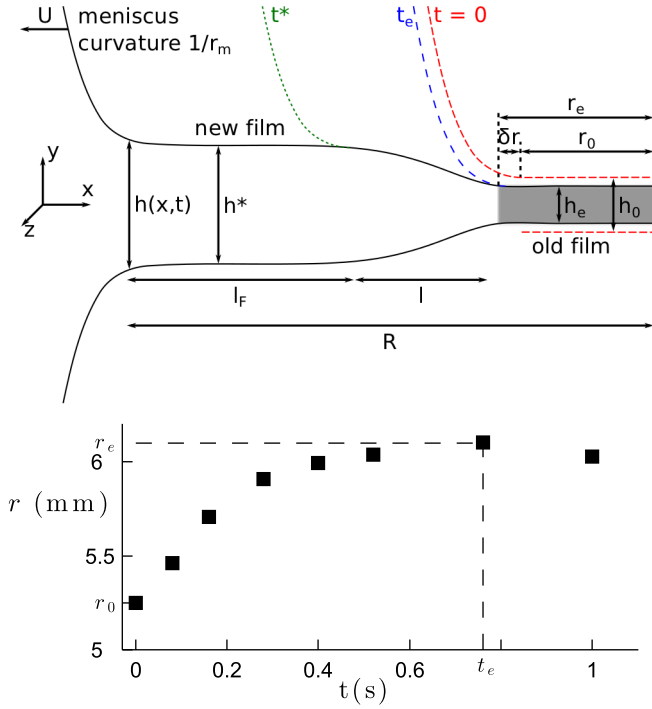| Solution	Composition	Surface tension γ (mN/m)
$T3$	TTAB (14.8 mmol/L = $3c_{\text{cmc}}$)	35
$T13$	TTAB (63.9 mmol/L = $13c_{\text{cmc}}$)	35
$T25$	TTAB (128 mmol/L = $25c_{\text{cmc}}$)	35
D	SLES (0.30), CAPB (0.15), and MAc (0.05) (in wt %)	23

FIG. 2 (color online).   Top: horizontal film profiles along a
radius, from the meniscus to the film center, at different times.
The dashed and dotted lines are schematic representations of the
film at $t = 0$, initial time; $t = t_e$, end of the old film extension;
and $t = t^*$, end of the new film transient. The solid line is the
numerical result of Eq. (1) for a time $t > t^*$. Bottom: radius of
the old film r as a function of time for $U_s = 5$ mm/s and
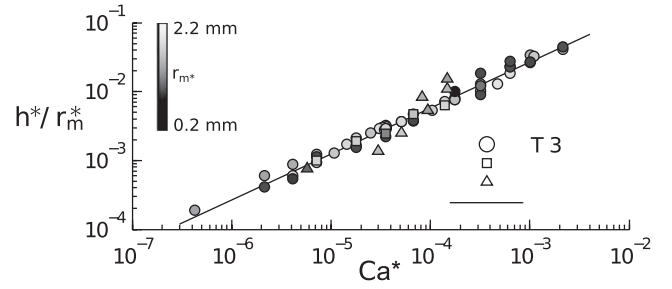solution T13. It saturates at $r_e = r(t_e)$.

FIG. 3.   Thickness h^* of the withdrawn film rescaled by the
Plateau border radius as a function of the Capillary number Ca*,
for different surfactant solutions. The gray value of each symbol
is proportional to r_m^*, from 0.2 mm (black) to 2.2 mm (white).
Data collapse on Frankel's law (solid line): $h_F/r_m^* = 2.68$Ca$^{*2/3}$.

Frankel's theory predicts the steady state shape of the
film $H_F(X)$ by setting $\partial_t H_F = 0$ in Eq. (1) and imposing
$H_F(X \to +\infty) = 1$. On the meniscus side ($X \to -\infty$), the
curvature of this solution reaches the constant value 0.643.
Matching with the meniscus curvature $1/r_m$ imposes
Frankel's law $h_F = 2.68 r_m$ Ca$^{2/3}$.

We solved the time-dependent equation, using as an
initial condition a profile with the required curvature at
$X \to -\infty$ (that is maintained constant in time) and a
constant thickness $H_e < 1$ at $X \to +\infty$. A flat film of
thickness $H = 1$ emerges from the meniscus and connects
to the initial film through a well-defined transition region
of length l (defined as the length of the region encompass-
ing 90% of the height variation). The profile obtained
for $H_e = 0.3$ and $T = 20$ is plotted in Fig. 2 (top) for X
in the range [-8; 22]: with these values of the parameters,
$l = 8.9 r_m$ Ca$^{1/3}$. Numerics showed that the variation of l
with H_e (less than 20% in the range [0.2–0.8]) and T (less
than 1% in the range [15–30]) are well below our experi-
mental dispersion; hence, we compared all our experimen-
tal data with the previous expression, finding a good
agreement (Fig. 4).

These results indicate that both the steady state thickness
and the transition region of the new film exactly follow
Frankel's theory. Our data thus evidence that all the tested
solutions are able to generate incompressible interfaces.
This incompressibility is ensured by surface tension gra-
dients, mainly arising from variations in the surface excess
of surfactants Γ, which balance bulk viscous stresses. For
solution (D), these gradients form as soon as the interface
stretches, independently of the subsurface concentration.
In contrast, for (T) solutions, surface and bulk concentra-
tions equilibrate faster than the experimental time scale.
Surface tension gradients thus imply bulk concentration
gradients, which appear in our system because of confine-
ment effects: the film is thin enough that it does not contain
many more surfactants than the interfaces, and is thus
easily depleted [25]. It is also large enough that diffusion
from the Plateau border is negligible (the typical bulk
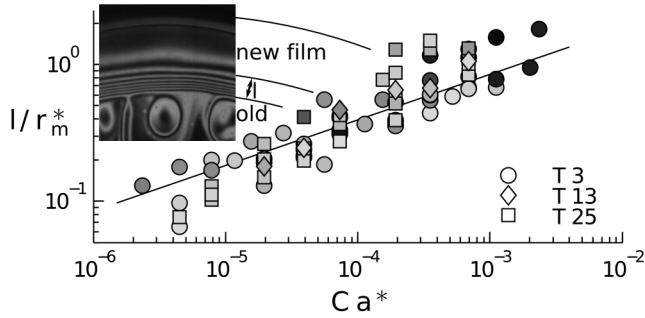diffusion time is 10^5 s). The observed rigidification is

this time. The best accuracy ($\pm 10\%$) on $r_m^* = r_m(t^*)$
was obtained by fitting the meniscus profile at $t = 0$
with its theoretical shape (taking into account corrections
due to axisymmetry and gravity) and by deducing r_m^* from
the meniscus volume conservation ($2\pi R r_m^2$ is constant,
neglecting the volume injected into the new film).
Finally, a fit of the form $h^* = K r_m^*$ Ca$^{*2/3}$ gives
$K = 2.7 \pm 0.1$.

The transition region is not described by Frankel's the-
ory, which only considers a steady state in the meniscus
frame. We thus developed an unsteady theoretical frame-
work based on the same assumptions to predict l [24]. The
problem is solved in the Plateau border frame, assuming
invariance in the z direction. A thin film of initial uniform
thickness $h_e[= h(t_e)]$ is pulled out of a meniscus of radius
r_m at a velocity U in the x direction (see Fig. 2, top). In the
lubrication approximation, and assuming that the interfa-
cial velocity is U everywhere, the dimensionless equation
of evolution written for the film half-thickness $H(X) =
h(x)/h_F$ is

$$\frac{\partial H}{\partial T} = -\frac{\partial}{\partial X}\left(H^3 \frac{\partial^3 H}{\partial X^3} + H\right), \quad (1)$$

with $X = 2x(3\text{Ca})^{1/3}/h_F$ and $T = 2t(3\text{Ca})^{1/3}U/h_F$.

FIG. 4. Length l of the transition region between the initial film and Frankel's film (rescaled by r_m^*), as a function of Ca^* (color coding is identical to Fig. 3). The solid line is the numerical prediction $l/r_m^* = 8.9 Ca^{*1/3}$. Inset: magnified view of the film featuring the interference pattern obtained with a monochromatic light. Each fringe increment corresponds to a thickness variation of 0.2 μm.

thus a striking illustration of the fact that surfactant behaviors do not exclusively depend on their intrinsic properties but also on the length and time scales involved [15,26].

The surface tension variation needed to pull the new film out of the Plateau border can be deduced from Frankel's calculation [21,27]

$$\frac{\delta\gamma}{\gamma} = \frac{\gamma_F - \gamma_P}{\gamma_P} = 3.8 Ca^{2/3}, \qquad (2)$$

where γ_P and γ_F are the surface tensions in the Plateau border (where it is equal to the equilibrium surface tension of the foaming solution) and at the end of the new film (i.e., in the old film). The old film surface tension must thus increase to allow extraction of Frankel's film, with a relative variation in the range $[10^{-4}$–$10^{-2}]$ for Ca in the range $[10^{-6}$–$10^{-3}]$.

The surface tension variation obeys $\delta\gamma = 2E_d\delta r/r_0$, with $\delta r = r_e - r_0$, as defined in Fig. 2. From Eq. (2), we find $\delta r/r_0 \sim 10^{-2}$ at $Ca = 10^{-3}$ for (D) solutions, which is consistent with the absence of measurable extension of the old film. In contrast, the E_d value measured in unconfined geometry is irrelevant for (T) solutions. It would lead in the same conditions to $\delta r/r_0 > 1$, which is not compatible with the measured extension.

To predict the area increase of the old film for (T) solutions, we must take into account the absorption of surfactant from the volume on the newly created interface, which lowers the bulk concentration in the film and leads to an increase of its surface tension. Let us consider a film of initial radius r_0 and thickness h_0, with a bulk concentration of surfactant $c_0 = \alpha c_{cmc}$ ($\alpha > 1$). We consider surfactants with small adsorption time, for which bulk and surface concentrations remain at equilibrium, and we assume that there is neither solution nor surfactant exchange with the Plateau border during the entire stretching. The surface tension is constant for $c > c_{cmc}$. Below the critical micelle concentration (cmc), γ decreases with c in a way that is
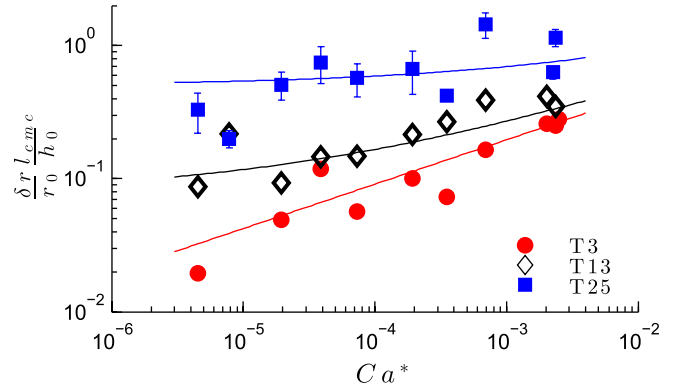

FIG. 5 (color online). Old film maximal extension $\delta r = r_e - r_0$ rescaled by $r_0 h_0/l_{cmc}$ as a function of Ca for the three TTAB solutions (averaged over several three series of various r_m for the $T25$, the error bars representing the standard deviation). Solid lines are the best fits of each curve with the prediction (3) using $K_\gamma = 0.15$ mN m^5/mol^2, $\alpha_3 = 1$, $\alpha_{13} = 1.3$, and $\alpha_{25} = 3.5$.

difficult to predict or measure with the required accuracy. A good agreement with the experimental data is obtained by assuming that $\gamma = \gamma_{cmc} + K_\gamma (c - c_{cmc})^2$ for $c < c_{cmc}$, which is the simplest function smoothly matching the condition $\gamma = \gamma_{cmc}$ for $c > c_{cmc}$. The required surface tension variation is thus obtained for a concentration variation $\delta c/c_{cmc} = 1 - \alpha - \sqrt{\delta\gamma/K_\gamma}/c_{cmc}$.

A surfactant mass balance then relates δc to δr. At first order in δr, $\delta r/r_0 = -h_0\delta c/(4l_{cmc}c_{cmc})$, where $l_{cmc} = \Gamma_{cmc}/c_{cmc} \approx 1$ μm. We used the fact that $\Gamma \approx \Gamma_{cmc} = 3.6 \times 10^{-6}$ mol/m^2 for TTAB [28]. Using Eq. (2), we obtain

$$\frac{\delta r}{r_0} = \frac{h_0}{4l_{cmc}} \left(\alpha - 1 + \sqrt{\frac{3.8\gamma_{cmc}}{K_\gamma c_{cmc}^2}} Ca^{1/3} \right). \qquad (3)$$

We plotted in Fig. 5 the old film extensions measured as a function of Ca, for the three solutions of type (T). The parameter α of Eq. (3) was fitted for each solution and a good agreement was obtained for $\alpha_3 = 1$, $\alpha_{13} = 1.3$, and $\alpha_{25} = 3.5$. These values are lower than the initial bulk concentrations ($\alpha = 3$, 13, and 25, respectively), which can be explained by the initial drainage process, known to reduce the concentration in the film [29,30]. The parameter K_γ was optimized globally for the three different solutions, with a best fit value $K_\gamma = 0.15$ mN m^5/mol^2.

In summary, we evidence in this Letter a homogeneous extension regime of surfactant films at small strain. This is in agreement with the linear relationship between stress and strain rate measured on surfactant films subject to small amplitude oscillatory forcing [11]. At larger strain, we evidence a second regime, which is perfectly described by a rigid interface model. This is the Frankel's regime, known to lead to a sublinear relation between stress and strain rate [6]. The elementary deformation that we study

[1] A. Britan *et al.*, Shock Waves **23**, 5 (2013).
[2] E. Del Prete, A. Chinnayya, L. Domergue, A. Hadjadj, and J.-F. Haas, Shock Waves **23**, 39 (2013).
[3] *Foam Engineering: Fundamentals and Applications*, edited by P. Stevenson (Wiley, New York, 2012).
[4] S. Cohen-Addad, R. Höhler, and O. Pitois, Annu. Rev. Fluid Mech. **45**, 241 (2013).
[5] A. M. Kraynik and M. G. Hansen, J. Rheol. **31**, 175 (1987).
[6] L. W. Schwartz and H. M. Princen, J. Colloid Interface Sci. **118**, 201 (1987).
[7] D. Buzza, C.-Y. Lu, and M. E. Cates, J. Phys. II (France) **5**, 37 (1995).
[8] N. D. Denkov, S. Tcholakova, K. Golemanov, K. P. Ananthapadmanabhan, and A. Lips, Phys. Rev. Lett. **100**, 138301 (2008).
[9] M. Durand and H. A. Stone, Phys. Rev. Lett. **97**, 226101 (2006).
[10] N. D. Denkov, S. Tcholakova, K. Golemanov, V. Subramanian, and A. Lips, Colloids Surf. A **282–283**, 329 (2006).
[11] S. Besson and G. Debrégeas, Eur. Phys. J. E **24**, 109 (2007).
[12] A. L. Biance, S. Cohen-Addad, and R. Höhler, Soft Matter **5**, 4672 (2009).
[13] B. Dollet and I. Cantat, J. Fluid Mech. **652**, 529 (2010).
[14] A.-L. Biance, A. Delbos, and O. Pitois, Phys. Rev. Lett. **106**, 068301 (2011).
[15] I. Cantat and B. Dollet, Soft Matter **8**, 7790 (2012).
[16] N. D. Denkov, V. Subramanian, D. Gurovich, and A. Lips, Colloids Surf. A **263**, 129 (2005).
[17] S. Marze, D. Langevin, and A. Saint-Jalmes, J. Rheol. **52**, 1091 (2008).
[18] N. D. Denkov, S. Tcholakova, K. Golemanov, K. P. Ananthpadmanabhan, and A. Lips, Soft Matter **5**, 3389 (2009).
[19] K. Golemanov, S. Tcholakova, N. D. Denkov, M. Vethamuthu, and A. Lips, Langmuir **24**, 9956 (2008).
[20] S. Besson, G. Debrégeas, S. Cohen-Addad, and R. Höhler, Phys. Rev. Lett. **101**, 214504 (2008).
[21] K. J. Mysels, K. Shinoda, and S. Frankel, *Soap Films: Study of Their Thinning and a Bibliography* (Pergamon, New York, 1959).
[22] J.-C. Géminard, A. Żywociński, F. Caillier, and P. Oswald, Philos. Mag. Lett. **84**, 199 (2004).
[23] J. M. Chomaz, J. Fluid Mech. **442**, 387 (2001).
[24] S. L. Cormier, J. D. McGraw, T. Salez, E. Raphaël, and K. Dalnoki-Veress, Phys. Rev. Lett. **109**, 154501 (2012).
[25] D. Quéré and A. de Ryck, Ann. Phys. Fr. **23**, 1 (1998).
[26] N. J. Alvarez, D. R. Vogus, L. M. Walker, and S. L. Anna, J. Colloid Interface Sci. **372**, 183 (2012).
[27] I. Cantat, Phys. Fluids **25**, 031303 (2013).
[28] J. R. Lu *et al.*, J. Phys. Chem. **96**, 10 971 (1992).
[29] A. A. Sonin, A. Bonfillon, and D. Langevin, Phys. Rev. Lett. **71**, 2342 (1993).
[30] C. J. W. Breward and P. D. Howell, J. Fluid Mech. **458**, 379 (2002).